Virology 305, 31–43 (2003)
doi:10.1006/viro.2002.1770

A Shine-Dalgarno-like Sequence Mediates in Vitro Ribosomal Internal Entry and Subsequent Scanning for Translation Initiation of Coxsackievirus B3 RNA

Decheng Yang,[1] Paul Cheung, Yuhua Sun, Ji Yuan, Huifang Zhang, Christopher M. Carthy, Daniel R. Anderson, Lubos Bohunek, Janet E. Wilson, and Bruce M. McManus

The MRL/iCAPTUR[4]E Center, Department of Pathology and Laboratory Medicine, University of British Columbia-St. Paul's Hospital, Vancouver, B. C., Canada

Received February 21, 2002; returned to author for revision July 10, 2002; accepted September 9, 2002

Translation initiation of coxsackievirus B3 (CVB3) RNA is directed by an internal ribosome entry site (IRES) within the 5′ untranslated region. However, the details of ribosome-template recognition and subsequent translation initiation are still poorly understood. In this study, we have provided evidence to support the hypothesis that 40S ribosomal subunits bind to CVB3 RNA via basepairing with 18S rRNA in a manner analogous to that of the Shine-Dalgarno (S-D) sequence in prokaryotic systems. We also identified a new site within both the 18S rRNA and the polpyrimidine-tract sequence of the IRES that allows them to form stronger sequence complementation. All these data were obtained from *in vitro* translation experiments using mutant RNAs containing either an antisense IRES core sequence at the original position or site-directed mutations or deletions in the polypyrimidine tract of the IRES. The mutations significantly reduced translation efficiency but did not abolish protein synthesis, suggesting that the S-D-like sequence is essential, but not sufficient for ribosome binding. To determine how ribosomes reach the initiation codon after internal entry, we created additional mutants: when the authentic initiation codon at nucleotide (nt) 742 was mutated, a 180-nt downstream in-frame AUG codon at nt 922 is able to produce a truncated smaller protein. When this mutation was introduced into the full-length cDNA of CVB3, the derived viruses were still infectious. However, their infectivity was much weaker than that of the wild-type CVB3. In addition, when a stable stem-loop was inserted upstream of the initiation codon in the bicistronic RNA, translation was strongly inhibited. These data suggest that ribosomes reach the initiation codon from the IRES likely by scanning along the viral RNA.

Key Words: IRES; Shine-Dalgarno sequence; ribosome; CVB3; cap-independent translation; RNA structure; initiation codon.

INTRODUCTION

The mechanism of translation initiation of coxsackievirus B3 (CVB3) is different from that of eukaryotic mRNA. This is largely due to differences in RNA structure. Eukaryotic cellular mRNA is organized in a monocistronic manner and its relatively short 5′ untranslated region (5′UTR) is capped with a 7-methylguanosine triphosphate structure. CVB3 genome, like other picornaviruses, is a positive polarity single-stranded RNA molecule encoding a large single polyprotein that is processed into more than 10 structural and nonstructural viral proteins after translation (Klump *et al.,* 1990; Minor, 1992). In addition, unlike eukaryotic mRNA, CVB3 RNA is not linked to a cap structure at its 5′ terminus; instead it is covalently linked to a viral-encoded small peptide, VPg. The 5′ UTR of CVB3, like other picornaviruses, is unusually long (741 nucleotides) and is organized into high order structures that regulate viral replication and pathogenicity (Agol, 1992; Haller *et al.,* 1995; Rinehart *et al.,* 1997; Bowles *et al.,* 1998; Gromeier *et al.,* 1999; Dunn *et al.,* 2000).

It has been reported that CVB3 and other picornaviruses use a different mechanism for the initiation of translation as compared to cellular mRNA (Hellen and Wimmer, 1995; Yang *et al.,* 1997; Graff and Ehrenfeld, 1998; Ishii *et al.,* 1999; Hinton and Crabb, 2001). In eukaryotic cells, the majority of the cellular mRNAs initiate translation via a 5′end- and cap-dependent ribosomal scanning mechanism. In such a model, a 40S ribosomal subunit binds initially to the cap structure along with other eukaryotic initiation factors (eIFs) to form a 43S complex at the 5′ end of mRNA and migrates along the mRNA chain with the assistance of other factors (eIF1 and eIF1A) until it encounters the initiation codon AUG. If the AUG codon occurs in the optimal sequence context (ACCAUGG), most, if not all, 43S subunits stop there; thus the AUG serves as a unique site for translation initiation (Hershey, 1991; Pestova *et al.,* 2001). By contrast, in the picornavirus, the 5′UTR is highly structured and the translation initiation has been shown to be mediated by internal binding of the ribosome on a specific sequence element of the 5′UTR, termed the internal ribosomal entry site (IRES) or ribosome lading pad (Jang *et al.,* 1988;

[1] To whom correspondence and reprint requests should be addressed at Cardiovascular Research Laboratory, University of British Columbia, St. Paul's Hospital, 1081 Burrard Street, Vancouver, B.C. Canada V6Z 1Y6. Phone: (604)-682–2344 ext. 62872; Fax: 604-806-8351. E-mail: dyang@mrl.ubc.ca.

0042-6822/02 $35.00

Jackson *et al.,* 1990; Pelletier and Sonenberg, 1988). Within the IRES sequence, there are two conserved elements, a polypyrimidine tract and the approximately 22 nts downstream AUG box, both of which are suggested to play an important role for ribosome internal binding (Pilipenko *et al.,* 1992; Scheper *et al.,* 1994). Our previous mutational analyses *in vitro* and *in vivo* have determined the IRES sequence element of CVB3 RNA and further mapped the 5′ and 3′ boundaries of the IRES (Yang *et al.,* 1997; Liu *et al.,* 1999). According to the picornaviral translation initiation model, the IRES directs binding of the small ribosomal subunit to the viral 5′UTR, independent of a cap structure at the 5′ terminus of the RNA (Jackson *et al.,* 1990; Pestova *et al.,* 1991). This mechanism of translation initiation is the so-called cap-independent ribosomal internal initiation. This kind of translation initiation has been also discovered recently in a minority of eukaryotic mRNAs that contain a long 5′UTR (Gan, *et al.,* 1998; Stoneley *et al.,* 2000).

The binding of ribosomes to the IRES element of the 5′UTR is a complicated interaction process. The details of such a mechanism are still unclear. The earliest investigation of this issue was conducted with prokaryotic mRNA, which is organized in a polycistronic manner. It has been reported that the prokaryotic ribosome binds to mRNA internally via basepairing between the Shine-Dalgarno (S-D) sequence of the mRNA and the 3′ end sequence of the 16S ribosomal RNA (Sprengart *et al.,* 1990). For picornaviruses, it has been suggested that the polypyrimidine stretch of the IRES element is an S-D-like sequence responsible for ribosome internal binding within the 5′UTR through sequence complementation with the 3′ terminal sequence of the 18S ribosomal RNA (Nicholson *et al.,* 1991; Pestova *et al.,* 1991; Pilipenko *et al.,* 1992; Le *et al.,* 1992). According to Scheper *et al.* (1994), the average number of potential basepairs between the 3′ end sequence of the 18S rRNA and the polypyrimidine tract is eight. However, for CVB3, only four continuous basepairs are present in this region. Thus, it is reasonable to postulate another region in the 5′UTR having longer complementation with the 18S rRNA.

In addition, according to the mutational analysis of the IRES of CVB3 and other members of the *Picornaviridae* family, the IRES is not located very close to the authentic initiation codon (Meerovitch *et al.,* 1991; RohII *et al.,* 1994; Trono *et al.,* 1988; Yang *et al.,* 1997). For example, the distance between the IRES sequence and the initiation codon in CVB3, poliovirus and hepatitis A virus is approximately 112, 131 and 45 nucleotides (nts) long, respectively (Yang *et al.,* 1997; Trono *et al.,* 1988; Brown *et al.,* 1991; Brown *et al.,* 1994). How does the ribosome complex reach the AUG start codon and initiate protein translation? This issue has long been controversial. In poliovirus, it has been suggested that ribosomes may reach the initiation codon by scanning the RNA after internal entry (Pelletier and Sonenberg 1988; Jackson *et al.,* 1990). For hepatitis A virus, it has been reported that ribosomes can enter directly at the downstream authentic initiation codon AUG in the 3′ terminus of the IRES (Brown *et al.,* 1994). For encephalomyocarditis virus, the authentic initiation codon is not selected by a scanning mechanism (Kaminski *et al.,* 1990; Kolupaeva *et al.,* 1998). How ribosomes reach the AUG start codon in CVB3 translation initiation remains unknown.

In this study, we have constructed bicistronic plasmids and full-length CVB3 mutants to test our hypothesis on the viral translation initiation. First, we generated five bicistronic mutants and tested whether an S-D-like sequence is involved in ribosome internal binding within the IRES. Our data gave an affirmative answer and further defined a new site within the 18S rRNA that allows potentially stronger baseparing with the S-D-like element of CVB3. Second, we created three bicistronic mutants by site-directed mutagenesis to test whether ribosomes could scan to reach the start codon after internal entry. Translation *in vitro* using these mutants demonstrated that ribosomes reached the initiation codon likely by scanning. To further test this hypothesis, two more bicistronic mutants were produced by insertion of a stable stem-loop just upstream of the authentic initiation codon to block ribosomal scanning. These mutations strongly inhibited translation of CVB3 RNA, indicating that ribosomes reach the authentic initiation codon likely by scanning after internal entry. However, since translation was not totally abolished, ribosome shunting might have occurred for certain ribosomes when they reached the inserted stable stem-loop. Finally, a full-length CVB3 mutant with a disabled authentic AUG codon at nucleotide (nt) 742 was constructed to test whether ribosome could continue scanning to reach the downstream in-frame AUG codon at nt 922 during CVB3 infection in HeLa cells. The obtained data further support the ribosome scanning mechanism.

RESULTS

Construction of mutants

Ten bicistronic plasmid mutants were constructed in three groups according to our specific aims. The first group contained five mutants. One was made by reverse insertion of the IRES core sequence (nts 530–630) at the original location (*Pst*I-Msc I site) and named p(SERI). The reversed IRES core DNA sequence was used to transcribe an antisense IRES RNA. The other four mutants were generated in two subgroups. The first subgroup has two mutants created by substitutions of five and six nts and named p(S5) and p(S6), respectively. The p(S5) decreased the number of base pairs between the S-D-like sequence and the 18S rRNA. However, the p(S6) enhanced such complimentarity. The second subgroup includes additional two mutants constructed by deletions

of 15 nts and 46 nts in the polypyrimidine tract and named p([130] 562–576) and p([130] 546–592), respectively. Since the expression of reporter gene (CVB3 P1) is under the control of the 5′UTR, mutational analysis within this region can identify *cis*-acting elements in CVB3 translation initiation. Thus, these five mutants were used to test whether an S-D-like sequence is involved in ribosomal internal binding within the 5′UTR (Fig. 2).

To determine whether ribosomes need to scan to reach the authentic initiation codon after internal entry within the 5′UTR, another three mutants in the second group were created by nt substitution within the AUG_{742} or AUG_{922} or both, and named p(AUG_{742}), p(AUG_{922}) and p(double), respectively (Fig. 3). Mutant p(AUG_{742}) disabled the authentic initiation codon at nt 742, such that the first available in-frame AUG downstream at nt 922 might serve as the initiation codon. If true, this mutation increased the distance between the IRES and the start codon from 112 nts to 292 nts, forcing ribosome subunits to migrate downstream to find the next available start codon at nt 922. This latter AUG has been suggested to be an initiation codon because in our previous studies the *in vitro* translation using wild-type bicistronic mRNA consistently produce an extra protein, which is smaller than P1. Mutant p(AUG_{922}) carrying a substitution (AUG to AAG) at the potential start codon AUG_{922} was used to test whether this mutation can abolish the extra smaller protein translation. Mutant p(double) carries two mutations at both AUG_{742} and AUG_{922}, and was used as a control.

To further confirm that the ribosomes reach the initiation codon by scanning, a third group of three more bicistronic mutants were generated by insertion of a stem-loop between the IRES and the initiation codon AUG_{742}, named p(S-L1), p(S-L2) and p(S-L3), respectively (Fig. 4). For mutant p(S-L1), a stem-loop insertion containing 48 nts was synthesized by PCR from stem-loop A (nts 3 to 50) of the CVB3 5′UTR. For mutant p(S-L3), a 99-nt insertion was manipulated from stem-loop C (nts 101 to 199) of the 5′UTR (Fig. 1A). These two stem-loops are very stable and served as obstacles to ribosome scanning along the viral RNA. To confirm that the introduction of a stem-loop structure at this position did not affect translation efficiency, an additional mutant was constructed by insertion of a stem-loop (55 nts) with lower stability (-25 kcal/mol) and used as a control.

Finally, to test whether the AUG_{922} can serve as an initiation codon during CVB3 infection, two full-length CVB3 constructs (one wild-type and one mutant) were generated (Fig. 5). The full-length CVB3 mutant was constructed by introducing a disabled AUG_{742} into the wild-type full-length CVB3 cDNA pCMV5(CVB3) and named pCMV5(AUG_{742}). These mutants were used in transfection of HeLa cells to substantiate whether mutated CVB3 can still generate infectious particles.

RNA secondary structure prediction

To test whether stem-loop insertion upstream of the initiation codon alters the original RNA folding pattern, we used the GCG program (University of Wisconsin) to predict the secondary structure of the altered sequences. No major change was found in the RNA folding pattern around the insertion site. The IRES core sequence region maintained the same secondary structure as that of the wild-type 5′UTR (Fig. 1B). The immediate downstream sequence is the inserted stem-loop. The 5′ and 3′ termini of the 5′UTR sequences are indicated by a double-circle.

In vitro transcription and translation

RNA transcripts (~3.6 KB) were synthesized under the direction of SP6 RNA polymerase and confirmed by denaturing agarose gel electrophoresis. All RNA transcripts are in correct size, indicating that mutations did not destabilize the RNAs (Fig. 2-4). *In vitro* translation of wild-type and mutant RNAs was conducted in rabbit reticulocyte lysates supplemented with HeLa cell extracts because the rabbit reticulocyte lysates do not contain all necessary factors for efficient cap-independent internal translation initiation of P1. Fig. 2B demonstrates the translation products of wild-type and mutant transcripts. All mutants demonstrated lower P1 translation efficiency than the wild-type RNA. The mutants p(Δ546–592) and p(Δ562–576) containing a 46-nt and a 15-nt deletion respectively at the polypyrimidine-tract region produced the lowest amount of protein, followed by mutants p(S5) and p(SERI). It is worth mentioning that the p(S5) only contains a 5-nt substitution aimed to destabilize the ribosome binding at the polypyrimidine-tract region, but it could strongly inhibit translation of P1, suggesting that the pyrimidine-rich motif plays a crucial role in ribosome entry. These data are in line with previous study on CVB1 (Iizuka *et al.,* 1991). Interestingly, a 6-nt substitution aimed to increase the number of basepairs between the S-D-like sequence and the 18S rRNA did not significantly increase the translation efficiency.

Translation of RNA transcripts containing mutated initiation codon is presented in Fig. 3. These mutants were used to verify whether the AUG_{922} downstream of the authentic start codon AUG_{742} can serve as an initiation codon and whether ribosomes can reach the AUG_{922} codon by scanning. Under optimal conditions, wild-type P1 RNA usually produces a 51 kDa (kDa) protein and a smaller protein (~47 kDa) (this smaller protein band is sometimes very weak). Mutant p(AUG_{742}) containing a disabled initiation codon at nt 742 only produced the smaller protein, and the 51 kDa P1 protein encoded by the open reading frame starting from nt 742 disappeared. The other mutant p(AUG_{922}) carrying a substitution at nt 922 produced a P1 of normal size, but failed to produce the 47 kDa protein as compared with the wild-type RNA.

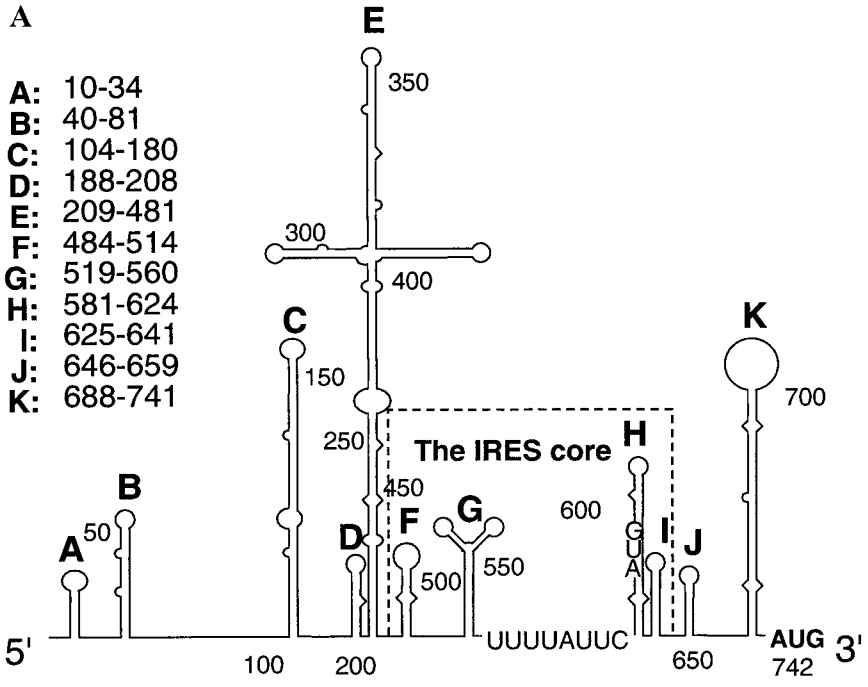

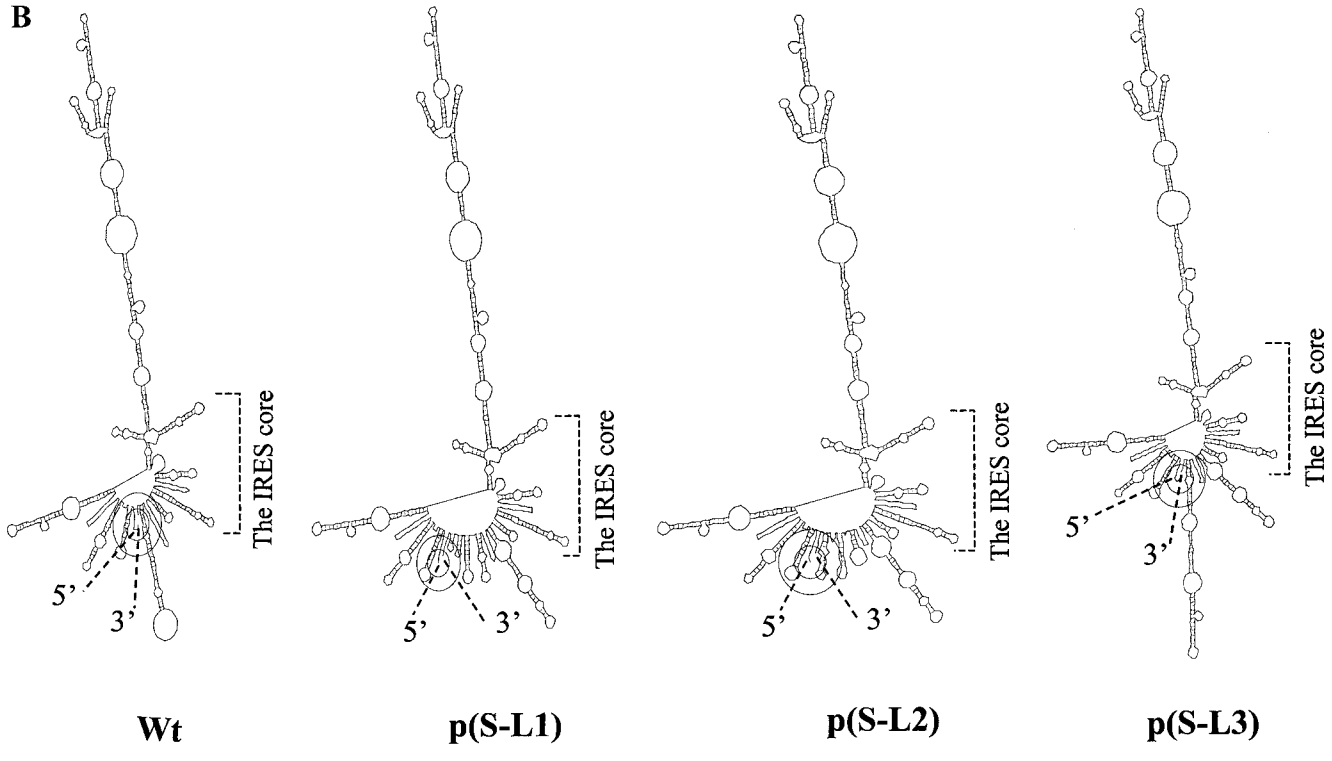

FIG. 1. Diagram of RNA secondary structure in the 5′UTR of CVB3. A) wild-type 5′UTR. The ranges of the numbers indicate the nts of respective stem-loop structures, which are labeled A through K. The IRES core, authentic initiation codon AUG at nt 742, conserved polypyrimidine tract and downstream AUG triplet are marked. B) The predicted secondary structure of mutant 5′UTRs containing stem-loop insertion upstream of the authentic initiation codon. The altered RNA sequences were re-predicted for the secondary structures by the same method used for prediction of wild-type 5′UTR. The wild-type (Wt) and mutant 5′UTRs are labeled. p(S-L1): containing a 48-nt insertion; p(S-L2): control mutant, containing a 55-nt insertion with lower stability; p(S-L3): containing a 99-nt insertion. The 5′ and 3′ termini of the 5′UTR are indicated by a double-circle. The secondary structure of the IRES core sequences remains unchanged in the altered sequences as compared with the wild-type 5′UTR. The insertion is at the immediately downstream of the IRES core.

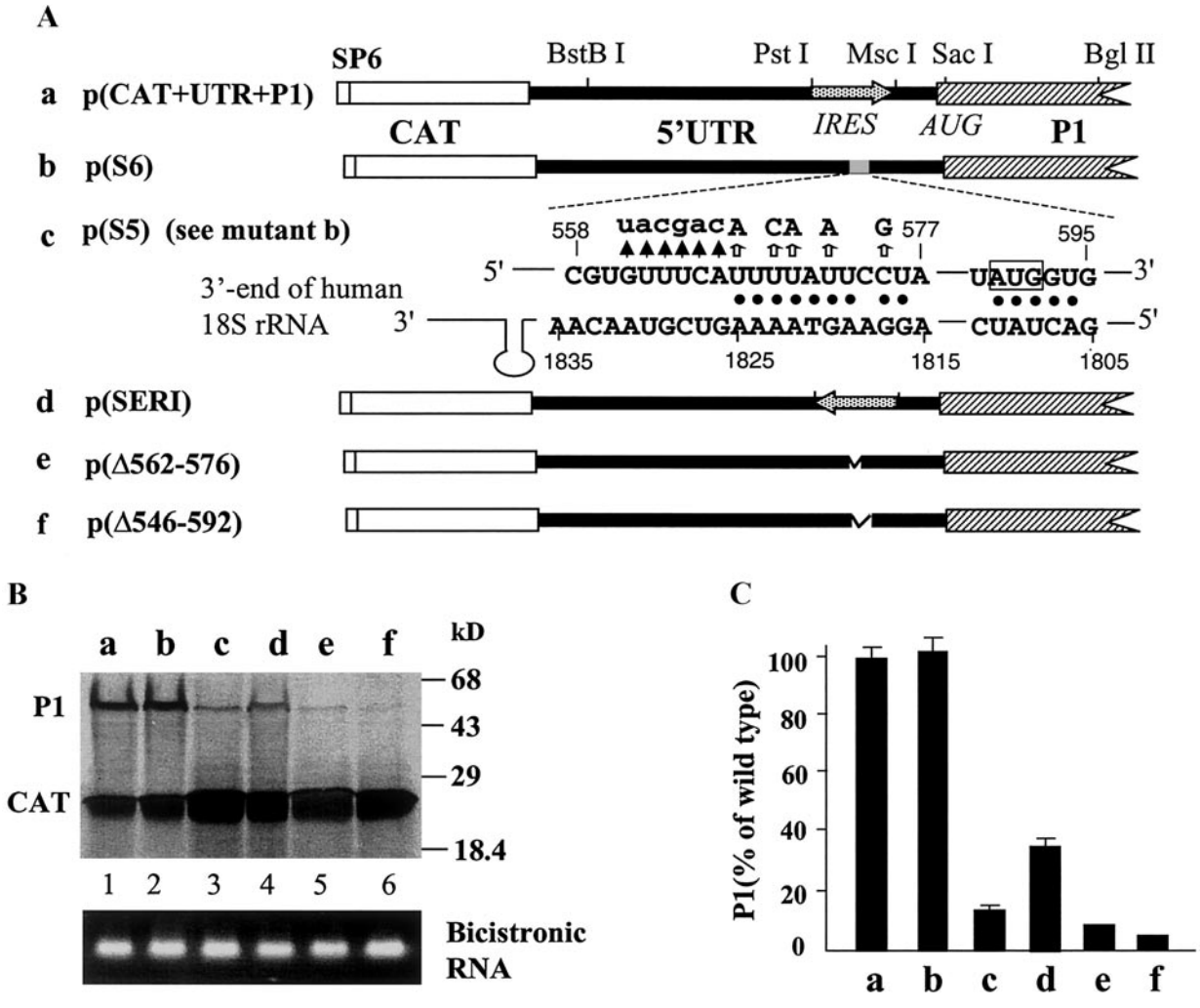

FIG. 2. *In vitro* translation using mutant RNAs to demonstrate that an S-D-like sequence is involved in the ribosome-template recognition. A) Map of the bicistronic plasmid p(CAT+UTR+P1) mutants used for synthesising RNAs by *in vitro* transcription. Locations of SP6 RNA polymerase promoter, chloroamphenical acetyltransferase (CAT) gene (open bar), 5′UTR (solid bar), truncated CVB3 P1 reporter gene (hatched bar) and the initiation codon are indicated. The restriction sites used for construction of mutants are labeled on the wild-type plasmid p(CAT+UTR+P1). The orientations of the IRES core sequence are indicated by big arrows. Base substitutions depicted by small open arrows represent mutations in p(S5). Base changes (lower case) pointed by solid arrows represent mutations in p(S6). The possible basepairs are denoted by dots. The conserved downstream non-initiation codon AUG is boxed. The numbering of the nts of 18S rRNA and CVB3 RNA are according to Le *et al.* (1992) and Kandolf *et al.* (1985), respectively. B) SDS-PAGE analysis of [^{35}S]methionine-labeled *in vitro* translation products. The intactness of bicistronic RNAs used for *in vitro* translation is demonstrated below the SDS-PAGE and labeled above each lane. C) Quantitation of translation products of P1 and CAT corresponding to those mutants in A. P1 protein expression was normalized with respect to CAT and presented as percent of P1 expression of wild-type RNA (Lane a). Lanes b-f: mutant RNAs. Data are mean ± SEM of three independent experiments.

Moreover, the control p(double) mutant did not produce any protein. These data suggest that the further downstream AUG is not competent for an initiation codon and the smaller 47 kDa protein was translated from AUG_{922}.

Ribosome scanning after internal entry was further tested by evaluating the translation of mutants that carry a stem-loop insertion upstream of the initiation codon. Fig. 4B shows that the translation of two mutants, p(S-L1) and p(S-L3), was strongly inhibited as compared with the wild-type and control RNAs p(S-L2), suggesting that ribosomal scanning was blocked by the stable stem-loop. However, since the stem-loop failed to abolish the translation completely, a small portion of ribosomes probably reached the start codon by shunting. Moreover, the inhibition of P1 (51 kDa) translation did not enhance the translation of the 47 kDa protein starting from AUG_{922}, suggesting that a second IRES is unlikely to be present immediately upstream of AUG_{922}.

Evaluation of the full-length CVB3 mutant

pCMV5(AUG_{742}) was used to transiently transfect HeLa cells using Lipofectamine reagent. The level of the viral capsid protein (VP1) expression and viral infectivity was evaluated by Western blot analysis and viral plaque assay, respectively. Figure 5B demonstrated that CVB3 VP1

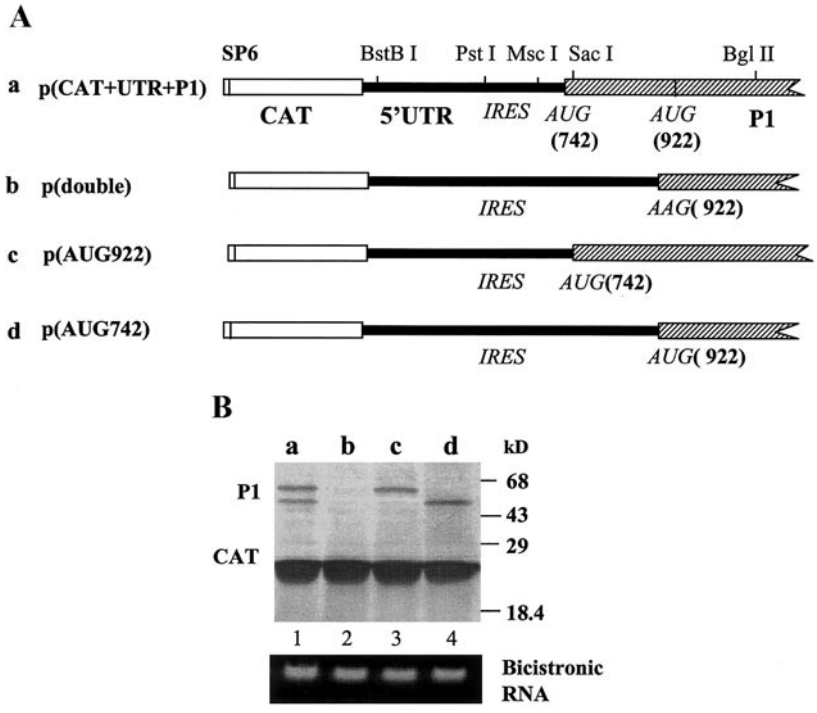

FIG. 3. *In vitro* translation using mutant RNAs to test whether ribosomal subunits need to scan to find the downstream initiation codon after internal entry and whether AUG_{922} can be recognised as a initiation codon. A) Map of the bicistronic plasmid p(CAT+UTR+P1) mutants. The restriction sites and the gene organisation of the plasmids are labeled in the same way as for Fig. 2A. B). Autoradiography of *in vitro* translation products labeled with [^{35}S]methionine. The intactness of bicistronic RNAs is shown and labeled above each lane. Lane 1: wild-type bicistronic RNA, producing CAT and two viral proteins (47 and 51 kDa). Lane 2: control mutant RNA containing two disabled initiation codons at nt 742 and 922 did not produce any P1 protein. Lane 3: mutant RNA changing the AUG to AAG at nt 922 failed to produce the 47 kDa protein, but still produced a 51 kDa protein. Lane 4: mutant RNA containing a disabled AUG_{742} could only produce a 47 kDa protein.

expression was significantly reduced but not totally abolished. Although the Western blot only showed a very weak band of VP1, the viral plaque assay demonstrated that a certain amount (85 pfu/ml) of infectious viral particles was produced in the mutated CVB3 cDNA-transfected HeLa cells. These infectious mutant viruses were further verified by RT-PCR and sequence determination, confirming that they are not revertants. These data indicate that the ribosome can scan along RNA and initiate translation at AUG_{922}.

DISCUSSION

It has long been known that ribosomes initiate translation in prokaryotic cells by a mechanism involving interactions between a S-D sequence of mRNA and the 3′ end sequence of the 16S ribosomal RNA (Sprengart *et al.,* 1990). This mechanism has been suggested to be suitable for picornaviruses. In other words, the pyrimidine-rich tract of the IRES in picornaviruses is a S-D-like sequence responsible for ribosome internal binding through basepairing with the 3′ end sequence of 18S rRNA (Pestova *et al.,* 1991; Pilipenko *et al.,* 1992). This basepairing model has been conceived largely on computer analysis of various picornavirus sequences and has only been tested in poliovirus by mutational analysis (Pilipenko *et al.,* 1992). In this study, we have tested this model in CVB3 using various mutants containing either a reversed IRES, base deletions, or site-directed mutations within the polypyrimidine tract and other regions. The reverse insertion resulted in the production of an RNA transcript containing the antisense sequence of the pyrimidine-rich tract. If ribosomal internal binding only relied on sequence complementation between the polypyrimidine tract and the 18S rRNA sequences, the mutation would block ribosome binding and in turn abolish translation of viral RNA. However, our results revealed that while translation efficiency of P1 was dramatically reduced, it was not abolished. This indicates that i) a S-D-like sequence is likely involved in the cap-independent ribosomal internal binding, but not as a unique factor in this interaction; ii) interaction between ribosome and the IRES may also be mediated by secondary structures (stem-loop) formed from palindrome sequences of the IRES. Because both the sense and antisense IRES sequences can form the same hairpin structures regardless of their orientations, they all play a role in assisting ribosome attachment. That is why the mutant p(SERI) could still produce a low level of P1 protein (Fig. 2).

Similar translation results were obtained when the other mutants containing deletions or substitutions were

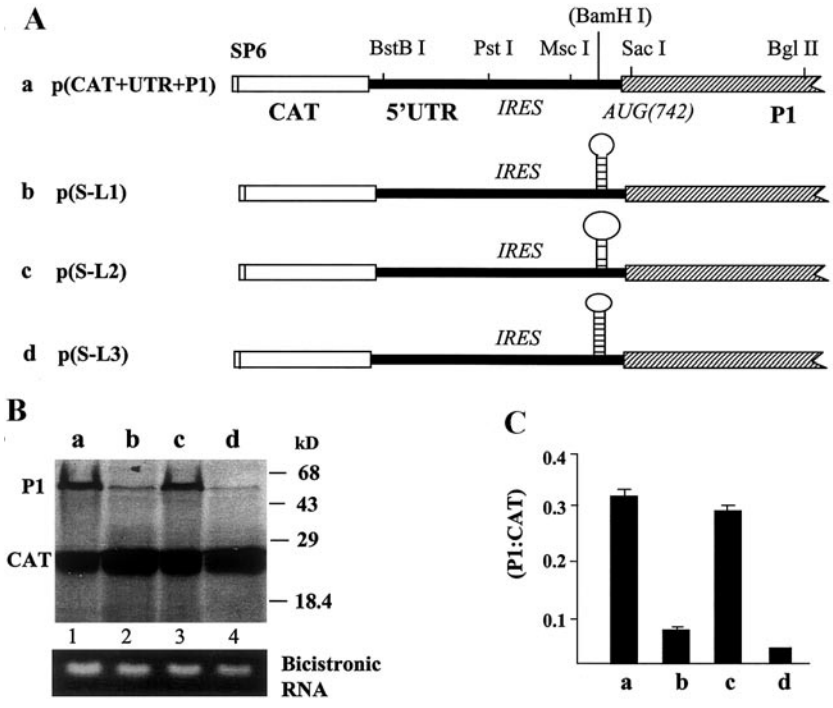

FIG. 4. *In vitro* translation using mutant RNAs to further confirm ribosomes initiate translation by scanning along RNA to recognise the authentic initiation codon. A) Map of the bicistronic plasmid p(CAT+UTR+P1) mutants used for synthesis of RNA. The restriction sites used for construction of mutants are labeled on the wild-type plasmid p(CAT+UTR+P1). *Bam*HI in parentheses is a new site created by PCR. The stem-loop insertions at the *Bam*HI site located upstream of the initiation codon are shown. B) SDS-PAGE analysis of *in vitro* translation products. The intactness of bicistronic RNAs is demonstrated. Lanes 1: wild-type bicistronic RNA. Lanes 2 and 4: mutant RNAs containing insertion of a stable stem-loop as described in Fig. 1. Lane 3: mutant RNA containing a non-stable stem-loop, which was used as a control. C) Quatitation of P1 and CAT translation products was performed as described in Fig. 2 and expressed as P1: CAT ratio. Note that the translation efficiency of the P1 gene was significantly decreased in Lanes 2 and 4, but not in Lane 3 as compared with that of wild-type RNA in Lane 1. Data are mean ± SEM of three independent experiments.

used. The deletion of the 46-nt sequence containing the polypyrimidine tract and the 23-nt downstream AUG box (DB), which is conserved in picornaviruses, caused the strongest inhibition of translation. Interestingly, a 15-nt deletion also significantly reduced the translation efficiency, suggesting that this region is critically important. This conclusion is further supported by the fact that a five-nt substitution in this region also causes a significant impairment of translation although it is weaker than that caused by the other two deletion mutants. In the selection of sites for mutagenesis aimed to decrease the complementarity, we chose a new region within the polypyrimidine tract as the S-D-like segment, a region differing from that of poliovirus. This is because if the basepairing pattern follows that of poliovirus, CVB3 RNA can only form four basepairs (i.e., nts 559–562) with the 18S rRNA. However, if the S-D-like sequence is shifted to a new location (nts 566 to 577), 9 basepairs can form with the 18S rRNA (nts 1816 to 1825) (Fig. 5B). Although this shifting decreases the level of complementarity between the 18S rRNA and the so-called DB sequence (around nt 595), it seems that the weakened basepairing at DB region will not affect the translation initiation since it has been reported that the DB sequence does not enhance translation initiation via basepairing with the 18S rRNA (O'Connor *et al.,* 1999; Moll *et al.,* 2001). In addition, Yusupava *et al.* (2001) have recently reported that the S-D sequence of prokaryotic mRNA, about 8 nts, can be directly observed at 7 A resolution within a large cleft between the head and the platform of the ribosome when using X-ray crystallography. Thus, the new site containing 9 nts is likely present in CVB3 RNA. These observations may explain why the 5-nt point mutation at the S-D-like region strongly inhibits translation of P1 and however mutant p(S6) that potentially forms 15 bp did not increase the amount of P1 product. The designed additional base pairs in the mutant may not occur in the natural structures of ribosome due to the limited space which only allows about 8 basepairs to form.

To determine how the ribosomes reach the initiation codon after internal entry, we created another mutant by the substitution of U with C within the authentic initiation codon AUG_{742}. This mutation shifted the initiation codon from nt 742 to the downstream first available in-frame AUG codon at nt 922. Therefore, the distance between the IRES and the start codon was increased by 180 nts. If ribosome can scan from the IRES in the 3′ direction after internal entry, it should use the downstream AUG_{922} as a start codon to synthesize a smaller P1 protein. Otherwise, no protein would be produced by the P1

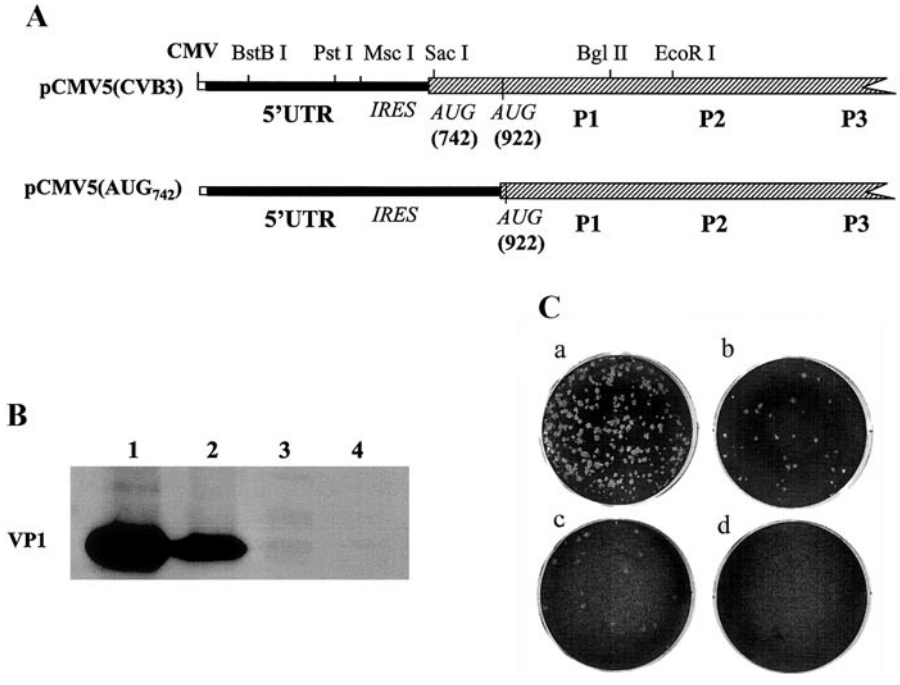

FIG. 5. Evaluation of full-length CVB3 mutant by transfection of HeLa cells to test whether AUG_{922} can serve as an initiation codon during CVB3 infection. A) Map of the full-length wild-type and mutant CVB3. Locations of CMV promoter, 5′UTR (solid bar), structural and non-structural proteins (hatched bar) and initiation codon AUGs are indicated. The restriction sites used for construction of mutants are labeled on the wild-type plasmid pCMV5(CVB3). B) Western blot analysis of CVB3 VP1 protein. Lane 1: HeLa cells infected with CVB3. Lane 2 and 3: HeLa cells transfected with wild-type and mutant CVB3 cDNA, respectively. Lane 4: HeLa cells transfected with pCMV5 vector-alone as a negative control. C) Plaque assay using supernatants derived from transfection of HeLa cells using wild-type and mutant cDNA, respectively. a-b: wild-type pCMV5(CVB3)-derived viral supernatant was diluted 1×10^4- and 1×10^5-fold and overlaid onto plates a and b, respectively. The viral titer obtained is 6.5×10^6pfu/ml; c: CVB3 mutant pCMV5(AUG_{742})-derived supernatant was overlaid on plate c without dilution. Viral titer obtained is 85 pfu/ml; d: Supernatant derived from pCMV5 vector-transfected HeLa cells was used as a negative control.

gene. We have demonstrated that a 47-kDa P1 protein was produced when using mutant RNA p(AUG_{742}) as a template. This protein is smaller than that (51 kDa) produced when using wild-type RNA as a template, suggesting that the ribosome needs to migrate from the IRES to reach the downstream AUG codon at nt 922 for translation initiation.

Now, the question remains as to how we prove that the AUG_{922} can be recognized as a start codon. To address this issue, first we checked the context sequence flanking the AUG according to the Kozak's (1989) rule, which indicates that whether an AUG is recognized as an initiation codon or not largely depends on its surrounding sequences. We have compared the sequence adjacent to AUG_{922} with that of AUG_{742}. Although not exactly the same, they are similar, suggesting that the AUG at nt 922 is a potential initiation codon for translation. Second, we created a mutant by changing the AUG at nt 922 to AAG and we also generated a double mutant by mutation at both AUG_{742} and AUG_{922}, which was used as a control in *in vitro* translation. It turned out that the mutant p(AUG_{922}) only produced the CAT and the 51 kDa P1, the smaller 47-kDa protein disappeared from the gel. However, the control did not produce any protein, indicating that AUG_{922} is likely the initiation codon for the 47-kDa protein. This conclusion is further supported by calculation of molecular mass according to the altered gene sequences. The new open reading frame starting from AUG_{922} is 180 nts shorter than the wild-type open reading frame starting from AUG_{742}. Such a shortening of the open reading frame will reduce the molecular mass of the new products to approximately 44.4 kDa, which is close to the molecular mass of ~47 kDa seen on the gel. In addition, there is no extra in-frame AUG codon downstream near nt 922. Therefore, it is unlikely that the ~47 kDa protein was synthesized by using another AUG as start codon. This has been further confirmed by our double mutant. This smaller protein was produced by a truncation of 60 amino acid residues from N-terminus of VP4. As mentioned earlier, this smaller protein was always produced in a small amount in our *in vitro* translation using wild-type bicistronic RNA. Thus, the more important question is whether the AUG_{922} can initiate translation during viral infection. Our experiments using a full-length CVB3 mutant in HeLa cell transfection generated an affirmative answer. It is interesting to note that the plaque sizes of wild-type and mutant viruses are similar. The possible reversion of mutant has been ruled out by sequence determination. As known from a number of reports, the molecular determinants of CVB3 virulence

are located in the 5′UTR and coding region including VP1 and VP2 (Lee *et al.,* 1997; Dunn *et al.,* 2000) but no report on VP4. Thus, truncation at the N-terminus of VP4 may not significantly decrease CVB3 virulence and in turn the plaque forming ability. However, since the translation efficiency and viral infectivity were very low, AUG_{922} may not be an active start codon in a non-pathogenic condition, at least in HeLa cells. Since CVB3 is a cardiotropic pathogen and causes myocarditis, whether this AUG codon can be activated in the infected heart needs to be studied.

Stable stem-loops have been used by Kozak (1986) to study the role of RNA secondary structures in regulation of translation. She concluded that small ribosomal subunits can readily melt structures that have a calculated Gibbs energy of formation of ~ -30 kcal/mol, but structures in the range of -50 kcal/mol resist melting. In the latter case, translation is inhibited 85–95%. We adopted this method of evaluation to further confirm ribosomal scanning along the 5′UTR to reach the start codon by using three mutants containing stem-loop insertions. Two of the three inserts are copies of stem-loops A and C of the CVB3 5′UTR, respectively (Fig. 1). These stem-loops are conserved among enteroviruses (Klinck *et al.,* 1998; Le *et al.,* 1992; Le and Maizel 1998) and very stable (Skinner *et al.,* 1989). The third insert in the control mutant is less stable. The Gibbs energy of these hairpin loops was calculated by the method of Zuker (1989) in the GCG program. The ΔG of stem-loop A, stem-loop C and the control are -72, -92 and -25 kcal/mol, respectively. According to Kozak's rule, these two stable insertions could stall ribosome migration. *In vitro* translation data strongly support our prediction. However, it is worthwhile to note that the translation initiation was not completely abolished, indicating that some of the ribosomes might have reached the authentic AUG codon by another nonlinear scanning route, such as shunting, which was reported in DNA viruses (Pooggin *et al.,* 1999; Pooggin *et al.,* 2001). Ribosome shunting requires mRNA to possess a short open reading frame (sORF) preceding the stable stem-loop; also the distance between the stop codon of the sORF and the stem-loop is critical (Pooggin *et al.,* 1999). Although our CVB3 mutants have a stable stem-loop, the sORF starting from nt 590 does not stop at the upstream of the stem-loop at nt 735 but at the downstream (nt 791). Whether this RNA structure is able to lead to ribosome shunting needs to be investigated. However, whether or not ribosome shunting can occur in these mutants is unlikely to affect our conclusion on the scanning mechanism because the wild-type CVB3 RNA does not contain a stable stem-loop immediately downstream of the sORF.

The studies of ribosome scanning mechanisms in translation initiation are significant since one of our goals is to define potential targets for design of antisense oligonucleotides to block viral translation. Our findings have indicated that the sequence element between the IRES and the authentic initiation codon AUG_{742} is a rational target for such a goal to block ribosome scanning. This hypothesis has been verified by our recent studies on the design and evaluation of anti-CVB3 antisense oligonucleotide drugs specifically targeting this region (Wang *et al.,*2001).

MATERIALS AND METHODS

Construction of mutants

The bicistronic plasmid p(CAT + UTR + P1) was constructed previously (Yang *et al.,* 1997). This plasmid contains a CAT gene and the 5′UTR of CVB3 followed by a truncated P1 gene of CVB3. P1 contains four capsid protein genes, in the order from 5′ to 3′, VP4, VP2, VP3 and VP1. The CAT gene is translated by cap-dependent mechanism and serves as an internal control for *in vitro* translation; P1 is under the control of the 5′UTR and serves as a reporter for cap-independent internal translation initiation. This plasmid and the full-length cDNA of CVB3 (Kandolf and Hofschneider, 1985; Klump *et al.,* 1990) were used as starting material for construction of mutants.

All mutants were constructed in groups according to our specific aims. To test whether an S-D-like sequence is required for the ribosome-template recognition, five mutants were constructed. The first one is achieved by reverse insertion of the IRES core sequence at the original position. In brief, the wild-type p(CAT + UTR + P1) was digested with *Pst*I and *Msc*I. The putative core IRES element (100 nts long) and the vector containing the rest of the insert were isolated from agarose gels using a Geneclean kit (Bio 101) and blunt-ended with dNTPs and T4 DNA polymerase. These two fragments were religated and the orientation of the IRES insertion was determined by DNA sequencing. The other four mutants were made by PCR-mediated site-directed mutagenesis. Five primers (Table 1) were synthesized for construction of these four mutants. The first upstream primer (CVB546) was a 36-mer containing a *Pst*I site at its 5′ end. The first 21 bases of this primer could form basepairs with nts from 526 to 546 of the complementary strand, and then the following nts from the 22^{nd} base to the end of the primer could form basepairs with nts 593–607. The sequence complementation between primer and template forced the CVB3 sequence to form a loop containing 46 nts from nts 547 to 592, a sequence deleted during primer elongation. A similar primer (CVB562) was 51 nts long and could force the CVB3 sequence to delete a loop containing 15 nts during PCR. The remaining two upstream primers, CVB565 and CVB599, were 62 and 56 nts long respectively. They all contain a *Pst*I sit at their 5′ terminus and have five and six point mutations at the pyrimidine-rich tract, respectively. The downstream primer (CVB780) was designed

TABLE 1

Primers Used for Site-Directed Mutagenesis

Primer	Sequence[a]	Location[b]	Restriction site
CVB546	ACTCTGCAGCGGAACCGACTagTGACAATTGAGAGA	526–607	*Pst I*
CVB562	ACTCTGCAGCGGAACCGACTACTTTGGGTGTCCGTgaTACTGGCTGCTTATGGTGA	526–596	*Pst I*
CVB599	ACTCTGCAGCGGAACCGACTACTTTGGGTGTCCGT**TACGAC**TTTTATTCCTATACT	526–581	*Pst I*
CVB565	ACTCTGCAGCGGAACCGACTACTTTGGGTGTCCGTGTTTCA**A**T**CA**A**A**TC**G**TATACTGGCTGC	526–587	*Pst I*
CVB780	AGCATTCAGCCTGGTCTC	781–798	—
CVB742	TACTTGAGCTCCC**G**TTTTGCTGTAT	732–756	*Sac I*
CVB8	GCCTGTGGGTTGATCCCAC	8–27	—
CVB922	GTGAAAGATATCA**A**GATTAAATCAC	910–934	*EcoR V*
CVB2062	GTGTATAATAGTTCAAGA	2045–2062	—
CVB101	ACT**G**GATCCTAGAAGTAACAC	101–121	*BamH I*
CVB199	TAT**G**GATCCTCAGTCCGG	182–199	*BamH I*
CVB50	GCT**G**GATCCCAATGGGCCTG	31–50	*BamH I*
CVB20	AAA**GG**ATCCTGTGGGTTGAT	3–22	*BamH I*
ODN1	AGCGGATCCGTGCATTGCCACATTGATGCGTTCTCCGTTGGTGTAGTAGTACAAGCGGATCCTAT		*BamH I*

[a] 5′ to 3′, bold letters reflect nucleotide substitutions. Lower case letters indicate the position of nt deletions. The underlined sequences are restriction sites. For oligodeoxynucleotides (ODN), only the sense strand is listed.

[b] The range of numbers indicates the location of each primer on the genomic RNA of CVB3.

for use with all four upstream primers. Both PCR products were digested by *Pst*I and *Sac*I and used to replace the counterparts of the wild-type bicistronic plasmid.

To mutate the authentic initiation codon, three mutants were generated by PCR-mediated site-directed mutagenesis. The first mutant was constructed by substituting the base U with C in the authentic initiation codon AUG at nt 742 (AUG_{742}). The downstream primer (CVB742) for this mutant was designed to have a *Sac*I site at the 5′end and span from nts 732 to 756; the upstream primer (CVB8) covers the sequence from nts 8 to 27 (Table 1). The PCR product was digested with *Sac*I and *BstB*I and replaced the counterpart of the wild-type plasmid p(CAT + UTR + P1). The second mutant was produced by changing the downstream in-frame AUG triplet at nt 922 (AUG_{922}) to AAG, since this AUG_{922} codon may have the potential to compete for translation initiation with authentic start codon AUG_{742}. Briefly, two primers were synthesized. The upstream primer (CVB922) covers sequence from nts 910 to 934 containing an *Eco*R V site at the 5′ terminus. Also the primer changes the T at nt 923 to an A. The downstream primer (CVB2062) spans nts 2045 to 2062. The PCR product was digested with *Eco*R V and *Bgl*II and used to replace the counterpart of the wild-type plasmid p(CAT + UTR + P1). The third plasmid containing a double mutation was created by replacing the *Eco*R V-*Bgl*II fragment of the first mutant containing ACG_{742} with above PCR product predigested with the same enzymes. This mutant was used as a control.

To determine whether this AUG_{922} can be used as an initiation codon during viral infection, a full-length CVB3 mutant was constructed. To achieve this, we first cloned the wild-type full-length CVB3 into an eukaryotic expression vector pCMV5. Briefly, two restriction fragments, *Eco*RI-*Bgl*II and *Bgl*II-*Sal*I covering the entire CVB3 cDNA, were isolated separately from the original pCVB3/T7 plasmid by restriction digestion. The two DNA fragments were then ligated with pCMV5 vector pretreated with *Eco*RI and *Sal*I. The resultant plasmid pCMV5(CVB3) contains the full-length wild-type CVB3 cDNA and was used as a control in transfection. The full-length CVB3 mutant was generated by replacement of a *Pst*I-*Bgl*II fragment (nts 529-2042) with its counterpart carrying an AUG_{742} mutation isolated from the corresponding bicistronic plasmid mutant described above.

To further test whether ribosomes need scanning to reach the authentic initiation codon, two more mutants were generated by insertion of a stable stem-loop immediately upstream of the initiation codon. This stem-loop served to block ribosomal scanning in the 3′ direction. The stem-loops were obtained by manipulation of the very stable stem-loops A and C at the 5′ end of the CVB3 5′UTR (Yang *et al.,* 1997). The primers for synthesis of the stem-loops all contained a *Bam*HI site at the 5′ end. For stem-loop A, we used primers CVB20 and CVB50 and for stem-loop B, primers CVB101 and CVB199. The stem-loop locations within the 5′UTR are indicated in Table 1. For control of this experiment, an additional mutant was constructed by insertion of a stem-loop with lower stability. This cDNA insert was obtained by complementation of two synthesized 55-mer oligodeoxynucleotides (ODN1 and ODN2, Table 1). The DNA inserts were digested with *Bam*HI and inserted at the *Bam*HI site (at nt 735), created by PCR previously (Liu *et al.,* 1999), immediately upstream of the authentic initiation codon AUG_{742} of p(CAT + UTR + P1).

Manipulation of plasmid DNA of the above mutants was carried out by transformation of *E. coli* DH5α. PCR for creation of mutations was performed in a 50 μl volume for 30 cycles under the following conditions:

denaturation at 95°C for 30 s, annealing at 48°C for 2 min, and extension at 72°C for 30 s. The desired mutants were confirmed by DNA sequencing using Sanger's dideoxy chain termination method on an automated DNA sequencer (Sanger *et al.,* 1977).

In vitro transcription

Plasmid DNA was prepared by either a modified standard method (Yang *et al.,* 1997) or using a DNA purification column (Qiagen). One μg of plasmid DNA was linearized with *Bgl*II and purified by phenol/chloroform extraction and ethanol precipitation. Runoff *in vitro* transcription was performed with SP6 RNA polymerase in the presence of m^7GpppG (Boehringer Mannheim) as per manufacturer's instructions (Promega). Transcription products were treated with RNase-free DNase I at 37°C for 15 min, and the size and integrity of the transcripts were confirmed by denaturing formaldehyde-agarose gel electrophoresis.

Preparation of HeLa cell extract

HeLa cells (ATCC) were grown in Eagle's minimal essential medium supplemented with 10% fetal bovine serum. Cytoplasmic extracts were prepared from HeLa cells according to a previously described protocol (Molla *et al.,* 1991), with some minor modifications. The extracts were dialyzed against buffer A [90 mM KOAc, 1.5 mM $Mg(OAc)_2$, 1 mM dithiothreitol, 10 mM HEPES, pH 7.6] for 12 h at 4°C and treated with micrococcal nuclease (20 μg/ml of extract) at 20°C for 20 min. The extract was used directly to enhance *in vitro* translation or stored at -80°C in aliquots adjusted to 15% glycerol.

In vitro translation.

Equal molar amounts of RNA transcripts (0.5 μg) of wild-type or mutant plasmid were used in a 25-μl translation mixture containing 12.5 μl of rabbit reticulocyte lysates and 5 μl of HeLa cell extracts prepared above. The translation was carried out at 30°C for 1 h with the presence of 2.0 μl of [^{35}S]methionine (specific activity >1000 Ci/mmol, NEN), 20 U of RNasin (Promega) and 0.5 μl of amino acid mixture (minus methionine). Aliquots of [^{35}S]methionine labeled translation products (CAT and truncated P1 polyprotein) were analyzed by sodium dodecyl sulfate-12.5% polyacrylamide gel electrophoresis (SDS-PAGE). Gels were soaked in En^{3}hance (Dupont) prior to drying and exposure to Xomat-AR film (Eastman Kodak). To confirm that the bands in gels represented the CAT and truncated P1 gene products, aliquots of [^{35}S]methionine labeled translation products were immunoprecipitated with a 1:500 dilution of either rabbit antiserum to recombinant P1 protein containing VP4-VP2-VP3 or rabbit antiserum to CAT protein (5 prime to 3 prime, Inc.) following the method of Brown *et al.* (Brown *et al.,* 1991). After elution of the proteins from Sepharose beads (Pharmacia), the samples were analyzed by electrophoresis as mentioned above. The quantitation of P1 and CAT was performed by laser densitometric scanning of the bands and the values were normalized with respect to CAT as described previously (Yang *et al.,* 1997). The mean density of each lane was calculated from three independent experiments.

Transfection of HeLa cells

Subconfluent (70–80%) HeLa cell monolayers on six-well plates were transfected with full-length CVB3 mutant cDNA using Lipofectamine reagent as described in the manufacturer's protocol (Gibco BRL). Briefly, plasmid DNA (2 μg) were mixed with 8 μl of Lipofectamine in 200 μl of serum-free DMEM and incubated at room temperature for 30 min. After the monolayers were washed twice with the serum-free DMEM, the DNA-Lipofectamine complex was mixed with additional 0.8 ml of the same medium and overlaid onto the washed monolayers. The cells were incubated for 5 h at 37°C in a CO_2 incubator and then add 1 ml of DMEM with 20% FBS without removing the transfection mixture. After incubation continues for 19 h, the supernatant and cells were collected for plaque assay to determine virus titer and immunoassay to detect viral VP1 protein, respectively. HeLa cells transfected with wild-type CVB3 cDNA and pCMV5 vector-alone were used as controls.

Western blot analysis

HeLa cells were harvested 24 h post-transfection and CVB3 capsid protein VP1 was detected by Western blot analysis following the procedure described previously (Liu *et al.,* 1999). In brief, samples containing equal amounts of proteins were denatured at 95°C for 5 min in loading buffer and analyzed by 12% SDS-PAGE. The samples were then transferred onto a nitrocellulose membrane. The membrane was blocked with PBS-Tween 20 containing 5% nonfat milk at room temperature for 2 h and then incubated with 1:1000 diluted primary antibody against VP1 (Denka Seiken Co., Ltd.) at room temperature for 2 h. The membrane was washed and incubated with 1:2000 diluted secondary antibody (rabbit anti-mouse IgG conjugated with HRPO, Transduction Laboratories, USA). Signal detection was achieved by the enhanced chemiluminescence method as per the manufacturer's instructions (Amersham Pharmacia).

Viral plaque assay

The virus supernatants collected from HeLa cell monolayers were briefly centrifuged to eliminate the cell debris. One portion of the viral particles was used to isolate viral RNA for checking the stability of mutant by RT-PCR and sequence determination as described previously (Liu *et al.,* 1999). The remaining portion was used for viral plaque assay in six-well plates. Briefly, when

cells were ~85–90% confluent, equal amounts of diluted supernatant were inoculated into each well. One hour after infection, the inoculum was aspirated and cells in each well were overlaid with 2 ml of complete nutrient medium containing 0.7% warm agar. After incubation at 37°C for 2–3 days, cells were fixed with Carnoy's fixative and stained with 1% crystal violet solution for 5 min. The plates were washed and the plaques were counted. Supernatant from a wild-type CVB3 cDNA-transfected HeLa cell monolayer was used as a control. The experiment was repeated twice.

Computer prediction of RNA second structures

The altered RNA sequences containing a stem-loop insertion at nt 735 were re-predicted for secondary structures by the same method (GCG program of University of Wisconsin) used for prediction of the wild-type 5′UTR previously (Yang *et al.,* 1997). The Gibbs energy of these hairpin loops was calculated by the methods of Zuker (1989) and only those structures with the lowest predicted energy were selected.

ACKNOWLEDGMENTS

We thank Dr. Reinhard Kandolf, University of Tubingen, Germany for generously providing us the cDNA of CVB3. These studies have been supported by grants from the Canadian Institutes of Health Research (D.C.Y and B.M.M), the Heart and Stroke Foundation of B.C. and Yukon (D.C.Y and B.M.M.) and the St. Paul's Hospital Foundation (D.C.Y).

REFERENCES

Agol, V. I. (1992). The 5′-untranslated region of picornaviral genomes. *Adv. Virus Res* **40,** 103–179.

Bowles, N. E., and Towbin, J. A. (1998). Molecular aspects of myocarditis. *Curr. Opin. Cardiol.* **13,** 179–184.

Brown, E. A., Day, S. P., Jansen, R. W., and Lemon, S. M. (1991). The 5′ nontranslated region of hepatitis A virus RNA: Secondary structure and elements required for translation *in vitro. J. Virol.* **65,** 5828–5838.

Brown, E. A., Zajac, A. J., and Lemon, S. M. (1994). *In vitro* characterisation of an internal ribosomal entry site (IRES) present within the 5′ nontranlated region of hepatitis A virus: Comparison with the IRES of encephalomyocarditis virus. *J. Virol.* **68,** 1066–1074.

Dunn, J. J., Chapman, N. M. Tracy, S., and Romero, J. R. (2000). Genomic determinants of cardiovirulence in coxsackievirus B3 clinical isolates: Localization to the 5′ nontranslated region. *J. Virol.* **74,** 4787–4794.

Gan, W., Celle, M. L., and Rhoads, R. E. (1998). Functional characterisation of the internal ribosome entry site of eIF4G mRNA. *J. Biol. Chem.* **273,** 5006–5012.

Graff, J., and Ehrenfeld, E. (1998). Coding sequences enhance internal initiation of translation by hepatitis A virus RNA *in vitro. J. Virol.* **72,** 3571–3577.

Gromeier, M., Bossert, B., Arita, M., Nomoto, A., and Wimmer, E. (1999). Dual stem loops within the poliovirus internal ribosomal entry site control neurovirulence. *J. Virol.* **73,** 958–964.

Haller, A. A., Nguyen, J. C., and Semler, B. L. (1995). Minimum internal ribosome entry site required for poliovirus infectivity. *J. Virol.* **67,** 7461–7471.

Hellen, C. U. T., and Wimmer, E. (1995). Enterovirus genetics. *In* 'Human Enterovirus Infection'. (H. A. Rotbart Ed.), pp. 25–72. American Society for Microbiology, Washington, D.C.

Hershey, J. W. B. (1991). Translation control in mammalian cells. *Annu. Rev. Biochem.* **60,** 717–755.

Hinton, T. M., and Crabb, B. S. (2001). The novel picornavirus *Equine rhinitis* B virus contains a strong type II internal ribosomal entry site which functions similarly to that of Encephalomyocarditis virus. *J. Gen. Virol.* **82,** 2257–2269.

Iizuka, N., Yonekawa, H., and Nomoto, A. (1991). Nucleptide sequences important for translation initiation of enterovirus RNA. *J. Virol.* **65,** 4867–4873.

Ishii, T., Shiroki, K., Iwai, A., and Nomoto, A. (1999). Identification of a new element for RNA replication within the internal ribosome entry site of poliovirus RNA. *J. Gen. Virol.* **80,** 917–920.

Jackson, R. J., Howell, M. T., and Kaminski, A. (1990). The novel mechanism of initiation of picornavirus RNA translation. *Trends Biochem. Sci.* **15,** 477–483.

Jang, S. K., Krausslich, H.-G., Nicklin, M. J. H., Duke G. M., Palmenberg, A. C., and Wimmer, E. (1988). A segment of 5′ nontranslated region of encephalomyocarditis virus RNA directs internal entry of ribosomes during *in vitro* translation. *J. Virol.* **62,** 2636–2643.

Kaminski, A., Howell, M. T., and Jackson, R. J. (1990). Initiation of encephalomyocarditis virus RNA translation: The authentic initiation site is not selected by a scanning mechanism. *EMBO J.* **9,** 3753–3759.

Kandolf, R., and Hofschneider, P. H. (1985). Molecular cloning of the genome of a cardiotropic coxsackie B3 virus: Full-length reverse-transcribed recombinant cDNA generates infectious virus in mammalian cells. *Proc. Natl. Acad. Sci. USA.* **82,** 4818–4822.

Klinck, R., Sprules, T., and Gehring, K. (1998). Structural conservation in RNA loops III and VI of the internal ribosome entry sites of enteroviruses and rhinoviruses. *Biochem. Biophys. Res. Commu.* **247,** 876–881.

Klump, W. M., Bergmann, I. Muller, B. C., Ameis, D., and Kandolf, R. (1990). Complete nucleotide sequence of infectious coxsackievirus B3 cDNA: Two initial 5′ uridine residues are regained during plus-strand RNA synthesis. *J. Virol.* **64,** 1573–1583.

Kolupaeva, V. G., Pestova, T. V., Hellen, C. U. T., and Shatsky, I. N. (1998). Translation eukaryotic initiation factor 4G recognises a specific structural element within the internal ribosome entry site of encephalomyocarditis virus RNA. *J. Biol. Chem.* **273,** 18599–18604.

Kozak, M. (1986). Influence of mRNA secondary structure on initiation by eukaryotic ribosomes. *Proc. Natl. Acad. Sci. USA.* **83,** 2850–2854.

Kozak, M. (1989). Context effects and inefficient initiation at non-AUG codons in eucaryotic cell-free translation systems. *Mol. Cell. Biol.* **9,** 5073–5080.

Lee, C., Maull, E., Chapman, N., Tracy, S., and Gauntt, C. (1997). Genomic regions of coxsackievirus B3 associated with cardiovirulence. *J. Med. Virol.* **52,** 341–347.

Le, S. Y., Chen, H. J., Sonenberg, N., and Maizel, J. V. (1992). Conserved tertiary structure elements in the 5′ untranslated region of human enteroviruses and rhinoviruses. *Virology.* **1991,** 858–866

Le, S. Y., and Maizel, J. V. (1998). Evolution of a common core in the internal ribosome entry sites of picornaviruses. *Virus Genes.* **16,** 25–38.

Liu, Z., Carthy, C. M., Cheung, P., Bohunek, L., Wilson, J. E., McManus, B. M., and Yang, D. C. (1999). Structural and functional analysis of the 5′ untranslated region of coxsackievirus B3 RNA: *in vivo* translational and infectivity studies of full-length mutants. *Virology* **265,** 206–217.

Meerovitch, K., Nicholson, R., and Sonenberg, N. (1991). *In vitro* mutational analysis of *cis*-acting RNA translational elements within the poliovirus type 2 5′ untranslated region. *J. Virol.* **65,** 5895–5901.

Minor, P. D. (1992). The molecular biology of poliovirus. *J. Gen. Virol.* **73,** 3065–3077.

Moll, I., Huber, M., Grill, S., Sairafi, P., Mueller, F., Brimacombe, R., Longei, P., and Bläsi, U. (2001). Evidence against an interaction between the mRNA Downstream box and 16S rRNA in translation initiation. *J. Bacteriol.* **183,** 3499–3505.

Molla, A., Paul, A. V., and Wimmer, E. (1991). Cell-free, de novo synthesis of polioviruses. *Science* **254,** 1647–1651.

Nicholson, R., Pelletier, J., Le, S. Y., and Sonenberg, N. (1991). Structural and functional analysis of the ribosomal landing pad of poliovirus Type 2: *In vivo* translation studies. *J. Virol.* **65,** 5886–5894.

O'Connor, M., Asai, T., Squires, C. L., and Dahlberg, A. E. (1999). Enhancement of translation by the downstream box does not involve base paring of mRNA with the penultimate stem sequence of 16S rRNA. *Proc. Natl. Acad. Sci. USA.* **96,** 8973–8978.

Pelletier, J., and Sonenberg, N. (1988). Internal initiation of translation of eukaryotic mRNA directed by a sequence derived from poliovirus RNA. *Nature* **334,** 320–325.

Pestova, T. V., Hellen, C. U. T., and Wimmer, E. (1991). Translation of poliovirus RNA: Role of an essential cis-acting oligopyrimidine element within the 5′ nontranslated region and involvement of a cellular 57–kilodalton protein. *J. Virol.* **65,** 6194–6204.

Pestova, T. V., Kolupaeva, V. G., Lomakin, I. B., Pilipenko, E. V., Shatsky, I. N., Agol, V. I., and Hellen, C. U. I. (2001). Molecular mechanisms of translation initiation in eukaryotes. *Pro. Natl. Acad. Sci. USA.* **98,** 7029–7036.

Pilipenko, E. V., Gmyl, A. P., Maslova, S. V., Svitkin, Y. V., Sinyakov, A. N., and Agol, V. I. (1992). Prokaryotic-like *cis* elements in the cap-independent internal initiation of translation on picornavirus RNA. *Cell* **68,** 119–131.

Pooggin, M. M., Fütterer, J., Skryabin, K. G., and Hohn, T. (1999). A short open reading frame terminating in front of a stable hairpin is the conserved feature in pregenomic RNA leaders of plant pararetroviruses. *J. Gen. Virol.* **80,** 2217–2228.

Pooggin, M. M., Fütterer, J., Skryabin, K. G., and Hohn, T. (2001). Ribosome shunt is essential for infectivity of cauliflower mosaic virus. *Proc. Natl Acad. Sci. USA* **98,** 886–891.

Rinehart, J., Gomez, R. M., and Root, R. P. (1997). Molecular determinants for virulence in coxsackievirus B1 infection. *J.Virol.* **71,** 3986–3991.

RohII, J. B., Percy, N., Ley, R., Evans, D. J., Almond, J. W., and Barclay, W. S. (1994). The 5′-untranslated regions of picornavirus RNAs contain independent functional domains essential for RNA replication and translation. *J. Virol.* **68,** 4384–4391.

Sanger, F., Nicklen, S., and Ceulson, A. R. (1977). DNA sequencing with chain-terminating inhibitors. *Proc. Natl. Acad. Sci. USA.* **74,** 5463–5467.

Scheper, G. C., Voorma, H. G., and Thomas, A. A. M. (1994). Basepairing with 18S ribosomal RNA in internal initiation of translation. *FEBS Letters* **352,** 271–275.

Skinner, M. A., Racaniello, V. R., Dunn, G., Cooper, J., Minor, P. D., and Almond, J. W. (1989). New model for the secondary structure of the 5′ non-coding RNA of poliovirus is supported by biological and genetic data that also show that RNA secondary structure is important in neurovirulence. *J. Mol. Biol.* **207,** 379–392.

Sprengart, M. L., Fatscher, H. P., and Fuchs, E. (1990). The initiation of translation in *E. coli*: apparent base pairing between the 16S rRNA and downstream sequences of the mRNA. *Nucleic Acids Res.* **18,** 1719–1723.

Stoneley, M., Chappell, S. A., Jopling, C. L., Dickens, M., MacFarlane, M., and Willis, A. E. (2000). **)**. C-myc protein synthesis is initiated from the internal ribosome entry segment during apoptosis. *Mol. Cell. Biol.* **20,** 1162–1169.

Trono, D., Andino, R., and Baltimore, D. (1988). An RNA sequence of hundreds of nucleotides at the 5′ end of poliovirus RNA is involved in allowing viral protein synthesis. *J. Virol.* **62,** 2291–2299.

Wang, A., Cheung, P., Zhang, H., Carthy C. M., Bohunek L., Wilson J. E., McManus B. M., and Yang, D. C. (2001). Specific inhibition of coxsackievirus B3 translation and replication by phosphorothioate antisense oligonucleotides. *Antimicrob. Agents Chemother.* **45,** 1043–1052.

Yang, D., Wilson, J. E., Anderson, D. R., Bohunek, L., Cordeiro, C., Kandolf, R., and McManus, B. M. (1997). *In vitro* mutational and inhibitory analysis of cis-acting translational elements within the 5′ untranslated region of coxsackievires B3: Potential targets for antiviral action of antisense oligomers. *Virology.* **228,** 63–73.

Yusupova, G. Z., Yusupov, M. M., Cate, J. H., Noller, H. F. (2001). The path of messenger RNA through the ribosome. *Cell.* **106,** 233–241.

Zuker, M. (1989). On finding all suboptimal foldings of an RNA molecule. *Science.* **244,** 48–52.